J|A|C|S ARTICLES

Published on Web 07/13/2009

Dynamics of Imidazolium Ionic Liquids from a Combined Dielectric Relaxation and Optical Kerr Effect Study: Evidence for Mesoscopic Aggregation

David A. Turton,*,† Johannes Hunger,‡ Alexander Stoppa,‡ Glenn Hefter,§ Andreas Thoman,|| Markus Walther,|| Richard Buchner,*,‡ and Klaas Wynne†

Department of Physics, SUPA, University of Strathclyde, Glasgow G4 0NG, U.K., Institute of Physical and Theoretical Chemistry, University of Regensburg, 93040 Regensburg, Germany, Chemistry Department, Murdoch University, Murdoch, W.A. 6150, Australia, and Department of Molecular and Optical Physics, Albert-Ludwigs-Universität Freiburg, 79104 Freiburg, Germany

Received May 1, 2009; E-mail: david.turton@phys.strath.ac.uk; richard.buchner@chemie.uni-regensburg.de

Abstract: We have measured the intermolecular dynamics of the 1,3-dialkylimidazolium-based room-temperature ionic liquids (RTILs) [emim][BF_4], [emim][DCA], and [bmim][DCA] at 25 °C from below 1 GHz to 10 THz by ultrafast optical Kerr effect (OKE) spectroscopy and dielectric relaxation spectroscopy (DRS) augmented by time-domain terahertz and far-infrared FTIR spectroscopy. This concerted approach allows a more detailed analysis to be made of the relatively featureless terahertz region, where the higher frequency diffusional modes are strongly overlapped with librations and intermolecular vibrations. Of greatest interest though, is an intense low frequency (sub-α) relaxation that we show is in accordance with recent simulations that have reported mesoscopic structure arising from aggregates or clusters—structure that explains the anomalous and inconveniently high viscosities of these liquids.

I. Introduction

To exploit the apparently great potential of room-temperature ionic liquids (RTILs) as solvents that offer both low environmental impact and product selectivity,[1,2] an understanding of the liquid structure, the microscopic dynamics, and the way in which the pertinent macroscopic properties, such as viscosity, thermal conductivity, ionic diffusion, and solvation dynamics depend on these properties, is essential. For the widely studied RTILs based on the imidazolium cation, these properties can be optimized by functionalizing the imidazolium ring as well as by choice of anion. The high viscosity of most RTILs would be a drawback in many applications, particularly so for large-scale synthesis, where high reaction rates are essential. An understanding of the interactions and structure of these liquids is therefore of paramount interest.

The structure of a neat RTIL is largely determined by a combination of long-range Coulombic forces, hydrogen-bonding interactions, and packing factors, as first demonstrated by NMR studies.[3,4] However, although RTILs have also been studied by scattering techniques,[5−8] which are highly informative on the local structure, there is little experimental evidence of the larger (mesoscopic) structure that has been suggested by computer simulations.[9−16]

RTILs have also been studied experimentally by calorimetry[17,18] and terahertz spectroscopy.[19] The subterahertz region, corresponding to intermolecular modes, has been investigated by Raman spectroscopy,[20,21] dielectric relaxation spectroscopy (DRS),[18,21−24] and optical Kerr effect (OKE) spectroscopy.[25−35]

† University of Strathclyde.
‡ University of Regensburg.
§ Murdoch University.
|| Albert-Ludwigs-Universität Freiburg.

(1) Chen, J. X.; Wu, H. Y.; Jin, C.; Zhang, X. X.; Xie, Y. Y.; Su, W. K. *Green Chem.* **2006**, *8*, 330–332.
(2) Migowski, P.; Machado, G.; Texeira, S. R.; Alves, M. C. M.; Morais, J.; Traverse, A.; Dupont, J. *Phys. Chem. Chem. Phys.* **2007**, *9*, 4814–4821.
(3) Avent, A. G.; Chaloner, P. A.; Day, M. P.; Seddon, K. R.; Welton, T. *Dalton Trans.* **1994**, 3405–3413.
(4) Dupont, J. *J. Braz. Chem. Soc.* **2004**, *15*, 341–350.
(5) Hardacre, C.; Holbrey, J. D.; McMath, S. E. J.; Bowron, D. T.; Soper, A. K. *J. Chem. Phys.* **2003**, *118*, 273–278.
(6) Triolo, A.; Russina, O.; Hardacre, C.; Nieuwenhuyzen, M.; Gonzalez, M. A.; Grimm, H. *J. Phys. Chem. B* **2005**, *109*, 22061–22066.
(7) Triolo, A.; Russina, O.; Bleif, H.-J.; Di Cola, E. *J. Phys. Chem. B* **2007**, *111*, 4641–4644.
(8) Kuang, Q. L.; Zhang, J.; Wang, Z. G. *J. Phys. Chem. B* **2007**, *111*, 9858–9863.
(9) Wang, Y. T.; Voth, G. A. *J. Am. Chem. Soc.* **2005**, *127*, 12192–12193.
(10) Wang, Y. T.; Voth, G. A. *J. Phys. Chem. B* **2006**, *110*, 18601–18608.
(11) Schröder, C.; Rudas, T.; Steinhauser, O. *J. Chem. Phys.* **2006**, *125*, 244506.
(12) Lopes, J.; Padua, A. A. H. *J. Phys. Chem. B* **2006**, *110*, 3330–3335.
(13) de Andrade, J.; Boes, E. S.; Stassen, H. *J. Phys. Chem. B* **2008**, *112*, 8966–8974.
(14) Habasaki, J.; Ngai, K. L. *J. Chem. Phys.* **2008**, *129*, 194501.
(15) Hardacre, C.; Holbrey, J. D.; Nieuwenhuyzen, M.; Youngs, T. G. A. *Acc. Chem. Res.* **2007**, *40*, 1146–1155.
(16) Bhargava, B. L.; Devane, R.; Klein, M. L.; Balasubramanian, S. *Soft Matter* **2007**, *3*, 1395–1400.
(17) Yamamuro, O.; Minamimoto, Y.; Inamura, Y.; Hayashi, S.; Hamaguchi, H. *Chem. Phys. Lett.* **2006**, *423*, 371–375.
(18) Rivera, A.; Rössler, E. A. *Phys. Rev. B* **2006**, *73*, 212201.
(19) Yamamoto, K.; Tani, M.; Hangyo, M. *J. Phys. Chem. B* **2007**, *111*, 4854–4859.
(20) Hayashi, S.; Ozawa, R.; Hamaguchi, H. *Chem. Lett.* **2003**, *32*, 498–499.

 10.1021/ja903315v CCC: $40.75

In general, DRS is limited to about 100 GHz, whereas the spectra of most RTILs are continuous up to several THz. Coverage of this entire region is therefore essential for an accurate analysis of even the low-frequency relaxational modes and here we have supplemented DRS by both time-domain terahertz spectroscopy[23] and Fourier transform far-infrared (FIR) spectroscopy to give an overall coverage from ca. 400 MHz to above 10 THz. We have then combined these measurements with OKE spectra that cover this frequency range in a single measurement and provide excellent signal-to-noise ratios in the terahertz region. Therefore, where previous spectroscopic studies of RTILs in the gigahertz to terahertz region have concentrated on either the low-frequency structural relaxation modes or the higher-frequency region where librational modes appear, we can fit the entire intermolecular spectrum with good precision.

Whereas DRS is sensitive to the derivative over time of the two-point time-correlation function[36] of the dipole moment μ,

$$S_{\mathrm{DR}}(\tau) \propto \frac{1}{k_{\mathrm{B}}T}\frac{\mathrm{d}}{\mathrm{d}\tau}\langle \mu(\tau)\,\mu(0)\rangle \qquad (1)$$

OKE measures the derivative over time of the two-point time-correlation function of the anisotropic part of the many-body polarizability tensor $\mathbf{\Pi}$ in the time domain

$$S_{\mathrm{OKE}}(\tau) \propto \frac{1}{k_{\mathrm{B}}T}\frac{\mathrm{d}}{\mathrm{d}\tau}\langle \Pi_{xy}(\tau)\,\Pi_{xy}(0)\rangle \qquad (2)$$

Both OKE and DR spectroscopies are primarily sensitive to rotational motions and only weakly sensitive to translations through the collision-induced response, and although the two techniques are complementary for intramolecular modes (as Raman- or IR-active vibrations), this is generally not the case at lower frequencies in condensed phases, where the modes are, to some extent, concerted, that is, they arise from the cooperative motions of multiple particles. Therefore, although differences arise due to the moiety undergoing the relaxation, the measured dynamics will be in many respects similar, with the two techniques generally measuring the same modes with different intensities.[36,37] Consequently, comparison of the DR and OKE spectra allows better resolution of the broad overlapping modes, which is a particular challenge to all linear spectroscopy of this region. A specific difference between the two techniques arises for the special case of isotropic single molecule diffusional rotations for which the OKE (2nd rank) relaxation time constant is three times smaller than the (1st rank) DRS relaxation time constant.[37,38]

In applying this approach to a small cross-section of RTILs based on the 1,3-dialkylimidazolium ion (Figure 1), 1-*N*-ethyl-3-*N*-methylimidazolium dicyanamide ([emim][DCA]), 1-*N*-butyl-3-*N*-methylimidazolium dicyanamide ([bmim][DCA]), and 1-*N*-ethyl-3-*N*-methylimidazolium tetrafluoroborate ([emim][BF_4]), we demonstrate that the measured dynamics can be described by a common and therefore more meaningful model, while, additionally, the comparison of the DR and OKE spectra allows the identification of motions due to the presence of the mesoscopic structure that has been predicted for some RTILs by computer simulations.[9−16]

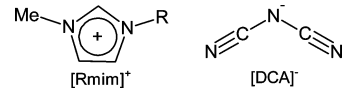

Figure 1. Ionic structures of the RTILs studied. $[Rmim]^+$ is either $[emim]^+$ (R = ethyl) or $[bmim]^+$ (R = butyl). The anion is either $[DCA]^-$ (dicyanamide) or $[BF_4]^-$.

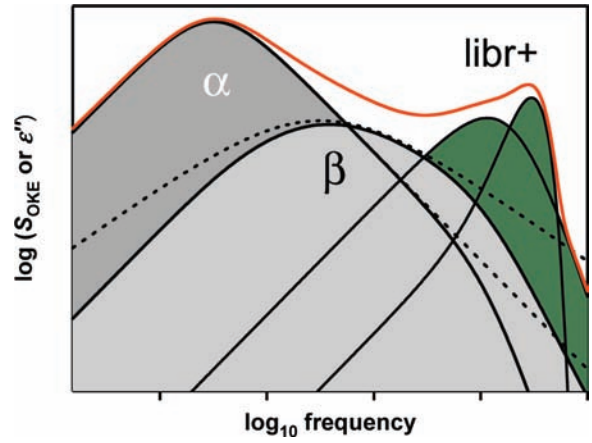

Figure 2. Simple model for molecular liquids shown in the frequency domain. The fundamental structural α relaxation (eq 4) at low frequency is accompanied by an unresolved β relaxation (β, eq 5). At higher frequencies, additional processes including librations and low-frequency intramolecular modes (libr+, eq 6 or 7) occur. The effect of inertial rise modifications and α termination can be seen by comparison with the unmodified functions (dotted). The resultant spectrum is also shown (in red). In this study, an intense band below the α relaxation (the sub-α mode) is also observed in the OKE spectrum.

II. Interpretation of the Intermolecular Spectrum

It has been shown previously[39] that a simple model of relaxation can be applied to the low-frequency spectra of *molecular* liquids. In this model (Figure 2), the α relaxation—the fundamental structural relaxation representing the decay of

(21) Rivera, A.; Brodin, A.; Pugachev, A.; Rössler, E. A. *J. Chem. Phys.* **2007**, *126*, 114503.
(22) Sangoro, J.; Iacob, C.; Serghei, A.; Naumov, S.; Galvosas, P.; Karger, J.; Wespe, C.; Bordusa, F.; Stoppa, A.; Hunger, J.; Buchner, R.; Kremer, F. *J. Chem. Phys.* **2008**, *128*, 214509.
(23) Stoppa, A.; Hunger, J.; Buchner, R.; Hefter, G.; Thoman, A.; Helm, H. *J. Phys. Chem. B* **2008**, *112*, 4854–4858.
(24) Hunger, J.; Stoppa, A.; Schrödle, S.; Hefter, G.; Buchner, R. *Chem. Phys. Chem.* **2009**, *10*, 723–733.
(25) Hyun, B. R.; Dzyuba, S. V.; Bartsch, R. A.; Quitevis, E. L. *J. Phys. Chem. A* **2002**, *106*, 7579–7585.
(26) Giraud, G.; Gordon, C. M.; Dunkin, I. R.; Wynne, K. *J. Chem. Phys.* **2003**, *119*, 464–477.
(27) Cang, H.; Li, J.; Fayer, M. D. *J. Chem. Phys.* **2003**, *119*, 13017–13023.
(28) Rajian, J. R.; Li, S. F.; Bartsch, R. A.; Quitevis, E. L. *Chem. Phys. Lett.* **2004**, *393*, 372–377.
(29) Li, J.; Wang, I.; Fruchey, K.; Fayer, M. D. *J. Phys. Chem. A* **2006**, *110*, 10384–10391.
(30) Shirota, H.; Castner, E. W., Jr. *J. Phys. Chem. B* **2005**, *109*, 21576–21585.
(31) Shirota, H.; Castner, E. W., Jr. *J. Phys. Chem. A* **2005**, *109*, 9388–9392.
(32) Shirota, H.; Wishart, J. F.; Castner, E. W., Jr. *J. Phys. Chem. B* **2007**, *111*, 4819–4829.
(33) Hunt, N. T.; Jaye, A. A.; Meech, S. R. *PCCP* **2007**, *9*, 2167–2180.
(34) Xiao, D.; Rajian, J. R.; Cady, A.; Li, S. F.; Bartsch, R. A.; Quitevis, E. L. *J. Phys. Chem. B* **2007**, *111*, 4669–4677.
(35) Castner, E. W., Jr.; Wishart, J. F.; Shirota, H. *Acc. Chem. Res.* **2007**, *40*, 1217–1227.
(36) Giraud, G.; Wynne, K. *J. Chem. Phys.* **2003**, *119*, 11753–11764.
(37) Fukasawa, T.; Sato, T.; Watanabe, J.; Hama, Y.; Kunz, W.; Buchner, R. *Phys. Rev. Lett.* **2005**, *95*, 197802.
(38) Turton, D. A.; Hunger, J.; Hefter, G.; Buchner, R.; Wynne, K. *J. Chem. Phys.* **2008**, *128*, 161102.
(39) Turton, D. A.; Wynne, K. *J. Chem. Phys.* **2008**, *128*, 154516.

correlation over the greatest spatial and temporal scales—is described, as a function of angular frequency, by the Debye function, $S_D(\omega) = 1/(1 + i\omega\tau)$, corresponding to an exponential decay in the time domain. Typically, the α relaxation is accompanied by a higher frequency β relaxation, which is associated with molecular "rattling-in-a-cage" or, more accurately, diffusional cage-constrained motions. The β relaxation is generally inhomogeneously broadened by the large-scale fluctuations associated with the α relaxation and can be modeled by the Cole−Cole function

$$S_{CC}(\omega) = \frac{1}{1 + (i\omega\tau)^{\beta}} \quad (0 < \beta < 1) \tag{3}$$

where the exponent β acts as a broadening parameter. Because the α relaxation imposes an upper limit on the lifetime of the inhomogeneity of the β relaxation (i.e., the components of the β relaxation cannot be slower than the structural α relaxation), the β relaxation is terminated such that it evolves into a Debye relaxation at times $t \geq \tau_\alpha$, where τ_α is the time constant of the α relaxation.

Frequently, the α and β relaxational modes are unresolved, in which case they may appear as a single Cole−Davidson function.[40] In more complex systems, such as supercooled and glass-forming liquids, where a greater degree of structure is apparent, the α relaxation may also be broadened. In such cases, the (time domain) stretched exponential (Kohlrausch−Williams−Watts) function[40] can be employed to introduce heterogeneity. As this function asymptotically approaches a simple exponential relaxation, it is more appropriate as a model of α relaxation than the Cole−Cole function.

To take into account the inertial response of the system to an impulse, the Debye-like functions can also be terminated at high frequency, enabling the relaxational modes to rise at a rate consistent with librational motions.[39,41] The modified Debye function can then be written as

$$S'_D(\omega) = \frac{1}{1 + i\omega\tau} - \frac{1}{1 + (i\omega + \gamma_{LIB})\tau} \tag{4}$$

where γ_{LIB} is the inertial rise rate. Similarly, the Cole−Cole function modified by both the inertial rise and α termination[39] becomes

$$S'_{CC}(\omega) = \frac{1}{1 + ((i\omega + 1/\tau_\alpha)\tau)^{\beta}} - \frac{1}{1 + ((i\omega + \gamma_{LIB} + 1/\tau_\alpha)\tau)^{\beta}} \tag{5}$$

The Cole−Cole function is often described as a distribution of Debye functions. These two modifications then simply impose physically reasonable upper and lower limits on the distribution without changing its fundamental character.

At higher frequencies, typically up to a few terahertz, modes appear that include librations (rocking or hindered rotations), short-range intermolecular vibrations, and low-frequency intramolecular modes, such as chain flexure. Generally, it is found that these modes can be satisfactorily fit by the Brownian (damped-harmonic) oscillator[26,42]

$$S_B(\omega) = \frac{{\omega_0}^2}{{\omega_0}^2 - \omega(\omega + i\gamma_B)} \tag{6}$$

where ω_0 is the resonant (undamped) angular frequency and γ_B the damping rate. In some cases, the Gaussian oscillator, which is generally defined as

$$\mathrm{Im}[S_G(\omega)] = \exp\left[-\frac{(\omega - \omega_0)^2}{{\gamma_G}^2}\right] - \exp\left[-\frac{(\omega + \omega_0)^2}{{\gamma_G}^2}\right] \tag{7}$$

appears to provide a better fit. The Gaussian line shape is generally interpreted as implying inhomogeneity of the mode, although linear spectroscopies such as OKE and DR cannot explicitly distinguish homogeneous and inhomogeneous line-broadening mechanisms. More complex functions such as the Kubo stochastic line shape, which can interpolate between the Gaussian and Debye functions, have been successfully applied to simple liquids. However, in general, where numerous modes are overlapped, increasing the number of parameters further would be meaningless.

For less-simple molecular liquids, supramolecular structure, such as aggregation or clustering, may give rise to one or more additional relaxation modes that are slower than, and consequently broaden, the single-molecule relaxations. For convenience, in the present context we refer to such a process as a sub-α mode and retain α relaxation to mean the fundamental *single* "*molecule*" relaxation.

III. Materials and Methods

The [bmim][DCA] was prepared from purified reactants as described in the literature.[43,44] [emim][BF_4] and [emim][DCA] were obtained from Iolitec (Denzlingen, Germany). Halide impurity levels were measured by potentiometric titration against Ag^+ to be <0.5% for [bmim][DCA] and <400 ppm for [emim][DCA]. While halide impurities in [emim][BF_4] were below the detection limit, an acidic proton (of mole fraction ≤0.01) was apparent in the ^{1}H NMR spectrum with a chemical shift of 6.5 ppm. All samples were dried under vacuum (<10^{-8} bar) at ∼40 °C for at least 7 days, yielding water contents <40 ppm by coulometric Karl Fischer titration. The dried salts were stored in a nitrogen-filled glovebox and all measurements were conducted under dry atmosphere.

Broadband dielectric spectra were obtained by a combination of data from a frequency-domain reflectometer using a Hewlett-Packard 85070M dielectric probe system based on a vector network analyzer (VNA) at 0.2−20 GHz,[45] two waveguide interferometers (IFMs) at 27−89 GHz,[46] and a transmission/reflection terahertz time-domain spectrometer (THz-TDS) at 0.3−3 THz.[47] All measurements were conducted at 25.00 ± 0.05 °C, except for the THz-TDS and FIR spectra, which were recorded at 25.0 ± 0.5 °C. Raw VNA data were corrected for calibration errors with a Padé approximation. For selected samples, two further IFMs at 8.5−17.5

(40) Angell, C. A.; Ngai, K. L.; McKenna, G. B.; McMillan, P. F.; Martin, S. W. *J. Appl. Phys.* **2000**, *88*, 3113–3157.
(41) Kalpouzos, C.; McMorrow, D.; Lotshaw, W. T.; Kenneywallace, G. A. *Chem. Phys. Lett.* **1988**, *150*, 138–146.
(42) Cho, M. H.; Du, M.; Scherer, N. F.; Fleming, G. R.; Mukamel, S. *J. Chem. Phys.* **1993**, *99*, 2410–2428.
(43) Fredlake, C. P.; Crosthwaite, J. M.; Hert, D. G.; Aki, S.; Brennecke, J. F. *J. Chem. Eng. Data* **2004**, *49*, 954–964.
(44) Holbrey, J. D.; Seddon, K. R. *Dalton Trans.* **1999**, 2133–2139.
(45) Buchner, R.; Hefter, G. T.; May, P. M. *J. Phys. Chem. A* **1999**, *103*, 1–9.
(46) Barthel, J.; Bachhuber, K.; Buchner, R.; Hetzenauer, H.; Kleebauer, M. *Ber. Bunsen-Ges. Phys. Chem.* **1991**, *95*, 853–859.
(47) Uhd Jepsen, P.; Fischer, B. M.; Thoman, A.; Helm, H.; Suh, J. Y.; Lopez, R.; Haglund, R. F. *Phys. Rev. B* **2006**, *74*, 205103.

GHz[46] were used to crosscheck the reliability of the VNA results and showed excellent agreement, within the precision of the instruments.

The FIR data were recorded from 0.9 to 12 THz on a Bruker Vertex 70 FTIR spectrometer with the liquids held between a pair of polymethylpentene (TPX) windows with a path length of 20 μm. An average of about 4000 scans was taken for each sample and a background spectrum taken from the windows alone was subtracted. Complex permittivity spectra were then derived by Kramers−Kronig transformation.[48]

The quantity measured in DRS is the total complex dielectric response $\hat{\eta}(\omega)$, which is related to the permittivity $\hat{\varepsilon}(\omega)$ by

$$\hat{\eta}(\omega) = \hat{\varepsilon}(\omega) - \frac{i\kappa}{\omega\varepsilon_0} = \varepsilon'(\omega) - i\left(\varepsilon''(\omega) + \frac{\kappa}{\omega\varepsilon_0}\right) \quad (8)$$

where $\varepsilon'(\omega)$ and $\varepsilon''(\omega)$ are respectively the frequency-dependent permittivity and dielectric loss, κ is the dc conductivity, and ε_0 the permittivity of free space. At low frequencies, $\hat{\eta}/\hat{\varepsilon}$ is the limiting factor and determines the minimum accessible frequency. At the high-frequency limit of this work, the value of ε' has become almost constant,[23] and ε'' has declined almost to zero, so that all intermolecular terahertz modes are well-defined within the spectral range. The composite DR spectra were resampled to evenly spaced logarithmic frequencies before fitting in order to give an equal weighting across the whole spectrum. This ensures that the two wings of a symmetrical function, such as a Debye or Cole−Cole, are weighted equally. As a measure of fit quality, the reduced error function χ^2 was simultaneously summed for ε' and ε''.[45]

The OKE technique is well established,[49] and our experiment has been described previously.[38,39] In this case, 800 nm wavelength pulses with an energy of 8 nJ at a repetition rate of 76 MHz were generated by a Coherent Mira-SEED oscillator. The beam was split into (90%) pump and (10%) probe beams, which were cofocused by a 10 cm focal length achromatic lens into a 2 mm path length quartz cuvette containing the sample. Precompensation in a homosil prism pair gave a 30 fs (fwhm) cross-correlation measured at the sample position. The employment of a 600 mm optical delay line with a resolution of 50 nm (0.33 fs) gave a time scale of 4 ns, resulting in a bandwidth extending down to 250 MHz, which can be interpolated by moderate zero-padding to <100 MHz. The step size around zero delay up to 0.5 ps was 10 fs, increasing logarithmically thereafter for a further 250 points. For each trace an average of at least 16 complete scans was taken, and before analysis the signals were resampled (by linear interpolation) to a linear time scale. A dual-chopper setup was used, to reduce noise arising from scattering in the sample and from Fresnel reflections at the sample windows. The sample temperature was controlled to 25.0 ± 0.1 °C by enclosing the cuvette in a close-fitting copper block heated by a pair of attached low-voltage electrical heaters.

The OKE data are fit in the time domain on linear scales, where the noise in the data is normally distributed. However, to allow the use of the Cole−Cole function, which has no time-domain analytical form, and reconvolution of the fit, the fit function was generated in the frequency domain and fit through a Fourier transform.[39]

IV. Results and Analysis

Figures 3−5 show the imaginary parts of the DR spectrum and the deconvoluted frequency-domain OKE signal for [emim][BF_4], [emim][DCA], and [bmim][DCA]. The DR spectra up to 2 THz have been presented in greater detail previously.[23] The apparently featureless region extending from ca. 30 GHz up to ca. 4 THz is shown by simulations to be comprised of cage-rattling motions consisting of librational modes, with a considerable contribution from intermolecular vibrations.[50,51] In our previous studies, this region has been fitted by a set of two or three Brownian oscillators.[23,26] Here the high signal-to-noise ratio of the OKE data and the comparison of the OKE and DR spectra provide very critical tests of the model.

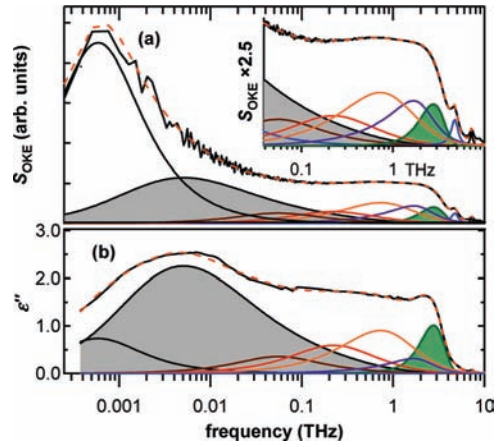

Figure 3. Spectra for [emim][BF_4] showing the total fit (dashed) and its component parts with the α relaxation (modified Cole−Cole function) and Gaussian oscillator shaded, to distinguish them from the Brownian oscillators and the sub-α relaxation: (a) OKE (imaginary part) with (inset) a vertical expansion and (b) dielectric loss, ε''. The fit parameters are shown in Table 1.

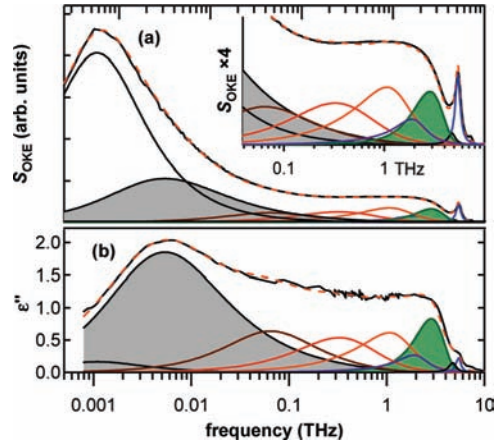

Figure 4. Spectra for [emim][DCA]: (a) OKE (imaginary part) and (b) dielectric loss, ε''. Details as for Figure 3.

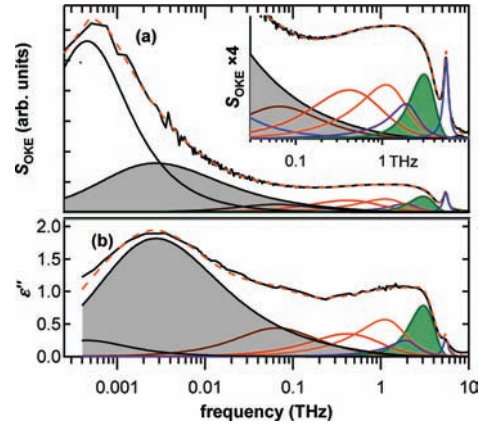

Figure 5. Spectra for [bmim][DCA]: (a) OKE (imaginary part) and (b) dielectric loss, ε''. Details as for Figure 3.

(48) Hunger, J.; Stoppa, A.; Thoman, A.; Walther, M.; Buchner, R. *Chem. Phys. Lett.* **2009**, *471*, 85–91.
(49) Smith, N. A.; Meech, S. R. *Int. Rev. Phys. Chem.* **2002**, *21*, 75–100.

Table 1. Fit Parameters for the Spectra in Figures 3−5[a]

	[emim][BF_4]				[emim][DCA]				[bmim][DCA]			
	A_{OKE} (au)	A_{DS}[b]	τ (ps)	β	A_{OKE} (au)	A_{DS}[b]	τ (ps)	β	A_{OKE} (au)	A_{DS}[b]	τ (ps)	β
sub-α	45	1.5	270		41	0.3	146		56	0.5	350	
α	23	7.9	61	0.65	18	5.0	44	0.8	32	6.0	90	0.69
	A_{OKE} (au)	A_{DS}[b]	$\omega_0/2\pi$ (THz)	$\gamma/2\pi$ (THz)	A_{OKE} (au)	A_{DS}[b]	$\omega_0/2\pi$ (THz)	$\gamma/2\pi$ (THz)	A_{OKE} (au)	A_{DS}[b]	$\omega_0/2\pi$ (THz)	$\gamma/2\pi$ (THz)
B_1	2.5	0.69	0.35	2.2	2.2	1.2	0.29	1.4	2.5	0.84	0.29	1.4
B_2	2.7	1.08	0.70	2.4	2.1	0.88	0.67	1.6	3.3	0.58	0.85	2.0
B_3	4.2	1.46	1.4	3.1	2.2	0.77	1.4	2.0	2.7	0.71	1.47	2.1
B_4	2.5	0.37	2.1	2.7	0.6	0.22	2.1	1.8	1.2	0.21	2.1	1.8
G	2.0	0.75	2.8	2.2	1.6	0.83	2.8	0.83	2.6	0.78	3.05	0.95
$*B_5$	2.5	0.01	4.8	0.95	0.07	0.02	4.8	1.0	0.5	0.04	5.5	0.88
$*B_6$	0.04	∼0	7.2	0.58	0.28	0.03	5.4	0.76	0.03	∼0	7.9	2.2
ε_∞		1.94				2.54				2.36		

[a] A_{OKE} and A_{DS} are the amplitudes of the OKE and DR modes; sub-α is the low-frequency Debye mode (eq 4); α is the (Cole−Cole) α relaxation (eq 5). The inertial rise rate γ_{LIB} in eqs 4 and 5 is relatively uncritical, having only a weak influence on the amplitudes of the terahertz modes, and was held constant at a value of 8 THz, consistent with the rise time (rather than the period) of the librational modes. B_n ($n = 1-6$) are the Brownian oscillators (eq 6); G is the Gaussian oscillator (eq 7); and $*B_n$ are high-frequency intramolecular modes. [b] The DR amplitudes are defined such that $\hat{\varepsilon}(\omega) = \varepsilon_\infty + A_{DS}S_i(\omega) + ...$, and the modified Debye and Cole−Cole functions are normalized by the generalized function $1/(1 + \tau/\tau_\alpha)^\beta - 1/(1 + (\tau/\tau_\alpha + \Gamma\tau)^\beta)$.

On this basis, the Gaussian oscillator, eq 7, is found to describe better the highly asymmetric high-frequency onset at ca. 3 THz. At higher frequencies, multiple underdamped intramolecular modes occur.

For each RTIL spectrum, six Brownian oscillators (eq 6) were employed in addition to the α relaxation (eq 5), the sub-α relaxation (eq 4), and the Gaussian oscillator (eq 7) (the real part of which was numerically approximated[52]). The same model then fits very closely both the OKE and DR spectra, including the stronger intramolecular modes up to 10 THz. The fit parameters are shown in Table 1.

We have shown previously[36,37] that a multi-Brownian oscillator model can be applied to both OKE and IR absorption spectra with a simple transformation in amplitudes. Here again, a single model can be seen to fit both OKE and DR spectra with just a change in amplitudes. Although the broad nature of the spectra in the terahertz region means that the choice of modes required for describing the intermolecular cage-rattling motions is still somewhat uncertain, the combination of the two techniques allows many inappropriate models to be eliminated. In most respects, the model for each liquid is very similar, suggesting that, in agreement with simulations,[50,51] the terahertz dynamics are dominated by the strong, many particle interactions, rather than by the specific nature of, the ions.

At higher frequencies, (underdamped) intramolecular modes appear. These have received little attention to date[26] and are generally unassigned. The DCA bending mode[35] appears at approximately 5.5 THz (184 cm^{-1}), and by comparison of the spectra for the three liquids, modes associated with the emim cation can be identified at approximately 4.75 and 7.2 THz (158 and 240 cm^{-1}). These are pronounced in the OKE spectra but appear only very weakly in the DR spectra.

However, the most surprising feature of these data occurs at low frequency, where, at ca. 1 GHz, a mode appears that is intense in the OKE spectra but so weak in the DR spectra that it would normally not be detected.[24] As will be shown below, this mode is best modeled by a Debye function. Normally, in both OKE and DR spectra, the lowest-frequency modes reflect rotational relaxation. For single molecule rotational diffusion, the macroscopic shear viscosity η can be related to the diffusivity D_{rot} through Stokes−Einstein−Debye theory, by $D_{rot} = k_BT/8\pi\eta R^3$, where R is the effective molecular radius. In the simplest cases of diffusional relaxation (e.g., symmetric tops) in which the dipole moment μ is coincident with the principal axis of the molecular polarizability ellipsoid Π, the (2nd rank) OKE signal relaxes 3 times faster than the (1st rank) DR signal.[37,38] Here, however, a simple qualitative comparison of the peak positions would suggest that the OKE relaxation is approximately five times *slower* than when measured by DR.

With no a priori model it is impossible to fit the low-frequency OKE peak unambiguously. Studies of similar ionic liquids have employed the Cole−Davidson function, which is well-established as an empirical model of α relaxation in supercooled and glass-forming liquids.[53,54] It is also frequently found that as the glass-transition temperature is approached, the mode resolves into a combination of a Debye function and a Cole−Cole function, where the latter may represent a Johari−Goldstein β relaxation.[53,54] However, the simple model described here (the Debye + Cole−Cole combination, with the former terminating the latter), is capable of reproducing this whole range of behavior and lends itself to a meaningful physical interpretation.

The second remarkable feature of these spectra is that if we apply this model to the OKE data, the Cole−Cole mode occurs at a very similar frequency to that in the DR spectrum. Since the slow components of the Cole−Cole mode cannot be slower than the sub-α relaxation, we now terminate the Cole−Cole function by the time constant of the sub-α relaxation, in contrast to the approach employed previously for DRS data alone.[24,55] A Debye function then accounts well for the OKE sub-α mode if the DR τ_α is used as the basis of the fit. The fit to the OKE signal measured in the time domain for [emim][DCA] (the least viscous of the present RTILs) is plotted on logarithmic axes in Figure 6, where it can be seen that the final decay ($t > 100$ ps) corresponds closely to a Debye function over almost 3 orders of magnitude in the OKE intensity. The DR spectrum can also be fit closely by the same model, albeit with a small amplitude for the sub-α relaxation.

(50) Schröder, C.; Haberler, M.; Steinhauser, O. *J. Chem. Phys.* **2008**, *128*, 134501.
(51) Shim, Y.; Kim, H. J. *J. Phys. Chem. B* **2008**, *112*, 11028–11038.
(52) Lether, F. G. *App. Math. Comput.* **1997**, *88*, 267–274.
(53) Blochowicz, T.; Tschirwitz, C.; Benkhof, S.; Rössler, E. A. *J. Chem. Phys.* **2003**, *118*, 7544–7555.
(54) Lunkenheimer, P.; Loidl, A. *Chem. Phys.* **2002**, *284*, 205–219.
(55) Hunger, J.; Stoppa, A.; Buchner, R.; Hefter, G. *J. Phys. Chem. B* **2008**, *112*, 12913–12919.

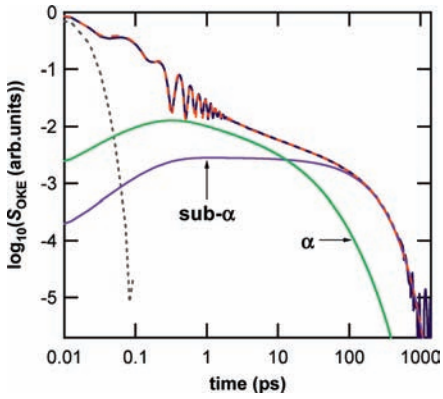

Figure 6. OKE data in the time domain for [emim][DCA] at 25 °C showing the overall fit (dashed) as described in the text and the two lowest-frequency components. The sub-α Debye relaxation shows the characteristic logarithmic scale curvature. Both the sub-α and α functions have the inertial rise modification, while the Cole−Cole α relaxation is additionally terminated by the sub-α mode. The instrument cross-correlation (dotted) is also shown.

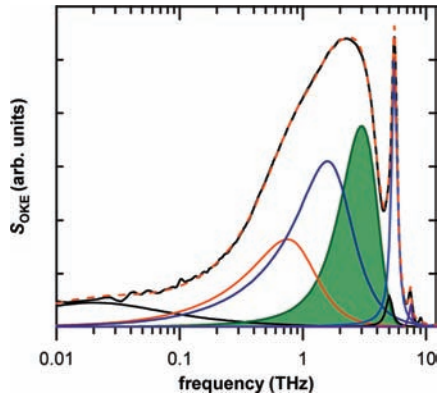

Figure 7. OKE spectrum for deeply supercooled [emim][DCA] at 180 K showing the overall fit (dashed) and its components: a Cole−Cole mode, two Brownian oscillators, a Gaussian oscillator (shaded) at the high-frequency onset of the librational band, and a further three Brownian oscillators. The fit parameters are shown in Table 2.

At lower temperatures the diffusional modes slow down[27,29] and we cannot study them with the current experimental bandwidth. However, consistent with other liquids exhibiting structure, RTILs are generally good glass-formers;[43,56] Figure 7 shows the OKE spectrum measured for deeply supercooled [emim][DCA] at 180 K (T_g = 169 K[57]). As the diffusional modes freeze out, the librational band becomes better defined. Compared with the room-temperature fit (Figure 4), the Gaussian mode shifts to slightly higher frequency but maintains the same damping rate, while the higher frequency Brownian librational modes broaden slightly. The lower frequency Brownian modes essentially freeze out, suggesting their nature is diffusional. A broad weak band remains below 0.1 THz that might be residual diffusional cage motions as implied by studies of ionic conductivity that report enhanced diffusivity in the glassy state.[21] Here the mode is fit by a Cole−Cole function, although this is quite approximate.

Table 2. Fit Parameters for [emim][DCA] at 180 K

mode	A (au)	τ (ps)	β
β	0.56	7.9	0.86
mode	A (au)	$\omega_0/2\pi$ (THz)	$\gamma/2\pi$ (THz)
B_1	1.0	0.98	1.4
B_2	1.7	1.94	2.4
G	1.9	3.0	1.0
$*B_3$[a]	0.04	5.04	0.7
$*B_4$[a]	0.31	5.5	0.7
$*B_5$[a]	0.013	7.5	0.4

[a] High-frequency intramolecular modes.

V. Discussion

The outstanding feature of the present measurements is undoubtedly the large signals in the OKE spectra that appear at considerably lower frequencies than the α relaxations measured by DRS. This is surprising, because simple theories predict that relaxations should be faster when measured by OKE. Although it is likely that the dipole moment and the polarizability ellipsoid are aligned differently, which would impact on the time constants through the molecular anisotropy, other studies[21,22] eliminate the possibility that the sub-α OKE mode occurs in the DR spectrum at lower frequencies than have been measured here. It is reasonable to conclude that OKE is sensitive to a sub-α mode that is only very weakly DRS-active.

The vast difference in the intensities observed for the low-frequency (sub-α) contribution in the OKE and DR spectra strongly implies that this process must correspond to a motion that causes a substantial change in the polarizability tensor without a simultaneous change in the macroscopic dipole moment, since there is only a weak contribution to the dielectric spectra. Computer simulations of [emim][BF_4] and [bmim][BF_4] have suggested that there is extensive stacking of the positively charged imidazolium rings with concomitant intercalation or coordination of the anions.[13] The presence of cation stacking is supported by recent DRS of RTIL mixtures,[58] where for [emim][BF_4] the dielectric data are compatible with large cation stacks, whereas for [emim][DCA] cation dimers sandwiched between two anions, similar to the structure suggested by MD simulations[13] for [emim][$AlCl_4$] and [bmim][$AlCl_4$] and by NMR spectroscopy[3] for [emim] halides, appear more likely. The sub-α mode implies a fluctuation in a large-scale aggregation, which introduces a major change in the polarizability with negligible influence on the macroscopic dipole. This suggests a mode with high symmetry, such as a simple breathing mode of a cation-stacked or micelle-like cluster. Simulations also show that, in these systems, there is a strong contribution from interaction-induced, translational motions, down to quite low frequencies.[11,50,51] This might reflect the inhibition of rotation by the aggregation or stacking.

A recent X-ray scattering study reported structure (nanoscale segregation) in dialkylimidazolium-based RTILs due to tail aggregation that increases with length of the alkyl substituents.[7] We cannot presently study these larger cations due to bandwidth limitations, but in line with MD simulations,[13] the present spectra suggest that structure exists even in RTILs with smaller (ethyl-substituted) cations. Although their origins might be quite different, cation-stacking and tail aggregation may well coexist. The OKE signal is not quantitative, but the magnitude of the

(56) Habasaki, J.; Ngai, K. L. *Anal. Sci.* **2008**, *24*, 1321–1327.
(57) MacFarlane, D. R.; Forsyth, S. A.; Golding, J.; Deacon, G. B. *Green Chem.* **2002**, *4*, 444–448.
(58) Stoppa, A.; Buchner, R.; Hefter, G. *J. Mol. Liq.* **2009**, in press (doi: 10.1016/j.molliq.2009.05.001).

sub-α mode implies that the clustering is quite extensive, in agreement with the simulations.[13] Such large-scale structure has been suggested as the source of very slow (∼1 s) exponential correlation decays in similar liquids.[8] These measurements were made by dynamic light scattering, which record time correlation of spatial density fluctuations on length scales greater than the probe wavelength. Such decays are sensitive to very large scale translational motion (or lifetime) of large clusters. Therefore, as we suggest that our measurements involve infracluster motions, it is not surprising that there should be a vast difference of time scale, even though the faster motions might be involved in the breakup and hence contribute to the lifetime of clusters.

The coincidence of the OKE and DR α relaxation times is still surprising but might be explained by recent MD simulations, which suggest that the mechanism of cation reorientation (in [emim][PF_6]) is dominated by large angle jumps rather than by rotational diffusion.[51] For jump reorientation, the OKE/DR relaxation time ratio is expected to be less than 3, and in the case of large jump angles (>109°), the OKE relaxation time can even be slower than that of DR.[59] Indeed, MD simulations for [emim][PF_6] find that the reorientation of a second rank observable can be up to 2 times slower than the first rank decay. We therefore suggest that the low symmetry of the liquids in combination with the jump mechanism can explain the agreement between the OKE Cole−Cole mode and the DR α relaxation.

Insight into structure can often be gained from a comparison of the measured α relaxation time constants with macroscopic viscosities. Although there are uncertainties in the available literature values for viscosity,[58,60] we showed recently that the effective volumes calculated through Stokes−Einstein−Debye theory for these liquids are extraordinarily small. This would suggest that single-molecule rotation is essentially decoupled from bulk viscosity, which is now unsurprising as this is characteristic of the hydrodynamic slip condition,[61] which has clear similarities with the jump model considered here. Viscosities of similar RTILs have also been studied previously, and association with stacking has been made.[30,62] Here it seems reasonable to say that the α relaxation time constant reflects jump reorientation, while shear viscosity is more dependent on the rearrangements of the stacked clusters.

VI. Concluding Remarks

In our previous DRS studies of imidazolium-based RTILs,[22,23,55] it was shown that the measured dynamics could be modeled by the combination of two low-frequency relaxational modes accompanied by typically two or three Brownian oscillators. A similar model was also applied in our previous OKE study, where particular attention was paid to the origin of the librational modes.[26] The present combination of OKE and dielectric spectra measured over an extended bandwidth shows that all data can be fit more accurately and reliably than was previously possible.

In the terahertz region, the signal-to-noise ratio of the OKE spectra is particularly high and the data show that there is a greater number of librational/intermolecular vibrational modes than previously detected. If simple functions (eqs 6 and 7) are employed, five modes are required to fit this region, although the degree of overlap still prevents an entirely unambiguous analysis. In fact, although there are distinct differences between the three liquids, this region of the spectrum is relatively flat and featureless, consistent with recent simulations.[11,50] In solid ionic conductors, this behavior is known as "nearly constant loss".[21] It manifests in the time domain approximately as a t^{-1} (power law) contribution to the decay and has frequently been identified as such in studies of glass-forming liquids and RTILs.[29] Here close scrutiny of the three spectra suggests that any similarity to a power law is coincidental. However, the extent to which it is appropriate to analyze this region through a set of independent modes is debatable, particularly for strongly interacting liquids. For now, this stands as a reasonable method of characterization.

The observation of an intense low-frequency mode in the OKE spectra is explained by the presence of mesoscale structure, while our finding of similar time constants for the OKE and DRS α relaxations supports recent claims from computer simulations,[58] suggesting that imidazolium cations reorient through large-angle jumps. The fact that a Cole−Cole function was required to fit the α relaxation band in the dielectric spectrum can now also be understood. Normally, if not accounted for by a simple Debye function, α relaxation can be modeled by a Cole−Davidson or stretched exponential function, as these tend to exponential relaxation at long times (i.e., they approach Debye behavior at low frequency). In the RTILs studied here, the lowest frequency motions are sub-α, which we have suggested correspond to mesoscopic clusters and hence inhomogeneity, which is reflected by the non-Debye nature of the α-relaxation.

Acknowledgment. The authors thank W. Kunz and H. Helm for laboratory facilities at Regensburg and Freiburg and acknowledge funding from the U.K. Engineering and Physical Sciences Research Council (EPSRC) and the Deutsche Forschungsgemeinschaft within Priority Program 1191.

JA903315V

(59) Böttcher, C. J. F. *Theory of electric polarisation*, 2nd ed.; Elsevier: Amsterdam, 1973; Vol. 1.
(60) Seddon, K. R.; Stark, A.; Torres, M. J. *Pure Appl. Chem.* **2000**, *72*, 2275–2287.
(61) Bauer, D. R.; Brauman, J. I.; Pecora, R. *J. Am. Chem. Soc.* **1974**, *96*, 6840–6843.
(62) Hunt, P. A. *J. Phys. Chem. B* **2007**, *111*, 4844–4853.